

# A LPV/ $\mathcal{H}_\infty$ Global Chassis Controller for Handling Improvements Involving Braking and Steering Systems

C. Poussot-Vassal<sup>1\*</sup>, O. Sename<sup>1</sup>, L. Dugard<sup>1</sup>

**Abstract**—To improve safety on commercial cars, a multivariable Global Chassis Controller (GCC) design, involving braking and steering systems is proposed. In case of emergency (e.g. loss of manoeuvrability), the GCC uses the braking system to handle the problem. But, in case of inefficiency of the braking system (e.g. due to low road adherence, large yaw rate error or actuator failure), detected by a braking efficiency measure, the proposed integrated controller activates the front steering system to handle the unlike vehicle dynamic. The proposed control structure is developed in the Linear Parameter Varying (LPV)  $\mathcal{H}_\infty$  framework.

## I. INTRODUCTION

### A. Motivations and structure of the paper

In most vehicle control design approaches, suspension, steering and braking control systems are synthesized independently to solve local problems. Then, the global communication and collaboration between each control structure (sensors, controllers and actuators) are achieved using empirical rules, derived thanks to the global knowledge of automotive engineers. But this kind of approach may lead to conflicting or inappropriate control objectives.

Then, the new trend in vehicle dynamic control (either commercial or heavy) is to synthesize multivariable controllers that are able to achieve both comfort and safety according to the vehicle situation (e.g. normal, dangerous or critical) and enhance performances using all the available actuators. This aim leads both industrial and academic to an increasing research in this area. Today, few interesting results concerning these points are available. In [1], a heavy vehicle Linear Parameter Varying (LPV) model is introduced with a scheduled robust control, involving suspensions and braking. In [2], an inverse model based control, involving an optimization procedure, is proposed. In [3], authors present an interesting nonlinear control law involving suspension and braking actuators for commercial cars. More recently, in [4], a nice model predictive approach (involving on-line optimization) using braking and steering actuators is proposed. In one of our previous studies [5], a LPV control structure involving suspensions and braking to improve comfort in normal situation and attenuate lateral acceleration in critical one, was proposed by monitoring the lateral load transfer.

In this paper, the aim is to propose a Global Chassis Controller (GCC), involving rear Electro-Mechanical Braking (EMB) and front Active Steering (AS) actuators, to enhance

vehicle handling and safety properties in critical and dangerous driving situations (e.g. large lateral acceleration and yaw rate error). To achieve the driving situation dependency, the proposed control approach is performed in the Robust ( $\mathcal{H}_\infty$ ) LPV framework where parameter dependency can be linearly introduced in the control design. Then, to achieve good braking and avoid slipping, the proposed GCC involves the Anti-locking Braking System (ABS) control mechanism recently developed by Tanelli et al. ([6]).

The interest of the proposed GCC is that, more than a simple controller, it provides a hierarchy to the actuators activation: when dangerous situation is detected, the GCC gives a torque reference to the braking system (that avoids slipping thanks to the ABS local controller), and if the braking system is not efficient enough and is not able to stabilize the vehicle (e.g. in case of low adherence or braking failure), the steering system is activated to handle the dynamical problem. Moreover, as long as it does not require any on-line optimization, the GCC structure also shows to be easy to implement on commercial cars. The originality of the proposed approach, compared to already existing ones, is that the controller can be fully integrated to the vehicle where local and efficient controllers already exist (e.g. ABS), and that, thanks to the LPV control structure, it adapts its performance objectives according to the driving situation and the actuators efficiency.

The structure of the paper is as follows. In Section I, introduction and vehicle parameters are given. Section II is devoted to the description of the full vehicle nonlinear model involved and of the considered actuators. Section III describes the LPV/ $\mathcal{H}_\infty$  GCC structure and its synthesis, and briefly gives the modified version of the ABS controller proposed in [6]. Simulations on the full vehicle nonlinear model are performed in Section IV to show the efficiency of the proposed method. Then, conclusions and results discussion are given in Section V.

### B. Notations and vehicle parameters

Throughout the paper, the following notation will be adopted: index  $i = \{f, r\}$  and  $j = \{l, r\}$  are used to identify vehicle front, rear and left, right positions respectively. Then index  $\{s, t\}$  holds for forces provided by suspensions and tires respectively.  $\{x, y, z\}$  holds for forces and dynamics in the longitudinal, lateral and vertical axes respectively. Then let  $v = \sqrt{v_x^2 + v_y^2}$  denote the vehicle speed,  $R_{ij} = R - (z_{us_{ij}} - z_{r_{ij}})$  the effective tire radius,  $m = m_s + m_{us_{fl}} + m_{us_{fr}} + m_{us_{rl}} + m_{us_{rr}}$  the total vehicle mass,  $\delta = \delta_d + \delta^+$  is the steering angle ( $\delta_d$ , the driver steering input and  $\delta^+$ ,

<sup>1</sup> GIPSA-lab, Control Systems Department (former LAG), INPG-CNRS-ENSIEG - Domaine Universitaire BP46, 38402 Saint Martin d'Hères - Cedex FRANCE

\* corresponding author: charles.poussot@gipsa-lab.inpg.fr

Symbol	Value	Unit	Signification
$m_s$	350	kg	suspended mass
$m_{us_{fj}}$	35	kg	front unsprung mass
$m_{us_{rj}}$	32.5	kg	rear unsprung mass
$I_x; I_y; I_z$	250; 1400; 679	kg.m <sup>2</sup>	roll, pitch, yaw inertia
$I_w$	1	kg.m <sup>2</sup>	wheel inertia
$l_f; l_r$	1.4; 1.4	m	front, rear axle
$l_f; l_r$	1.4; 1	m	COG-front, rear distance
$R$	0.3	m	nominal wheel radius
$h$	0.4	m	chassis height
$k_{fj}$	29500	N/m	front suspension stiffness
$k_{rj}$	20000	N/m	rear suspension stiffness
$c_{fj}$	1500	N/m/s	front suspension damping
$c_{rj}$	3000	N/m/s	rear suspension damping
$k_{t_{ij}}$	208000	N/m	tire stiffness
$c_{t_{ij}}$	10	N/m/s	tire damping
$b_t$	8.3278	—	lateral tire parameter
$c_t$	1.1009	—	lateral tire parameter
$d_t$	2268	—	lateral tire parameter
$e_t$	-1.1661	—	lateral tire parameter
$g$	9.81	m/s <sup>2</sup>	gravitational constant

TABLE I  
RENAULT MÉGANE COUPÉ PARAMETERS

the additional steering angle provided by steering actuator, see Section III) and  $T_{b_{ij}}$  the braking torque provided by the braking actuator (see Section III). Table I summarizes the model parameters, identified on a Renault Mégane Coupé, which is a sport oriented car [7].

## II. VEHICLE MODELING

### A. Dynamical equations

In this paper, a full nonlinear vehicle model is involved. It reproduces the vertical ( $z_s$ ), longitudinal ( $x$ ), lateral ( $y$ ), roll ( $\theta$ ), pitch ( $\phi$ ) and yaw ( $\psi$ ) dynamics of the chassis. It also models the vertical and rotational motions of the wheels ( $z_{us_{ij}}$  and  $\omega_{ij}$  respectively), the slip ratios ( $\lambda_{ij} = \frac{v_{ij} - R_{ij}\omega_{ij} \cos \beta_{ij}}{\max(v_{ij}, R_{ij}\omega_{ij} \cos \beta_{ij})}$ ) and center of gravity side slip angle ( $\beta_{cog}$ ) dynamics as a function of the tires and suspensions forces. The dynamical equations are given in equation (1), where  $F_{tx_i} = F_{tx_{il}} + F_{tx_{ir}}$ ,  $F_{ty_i} = F_{ty_{il}} + F_{ty_{ir}}$ ,  $F_{tz_i} = F_{tz_{il}} + F_{tz_{ir}}$  and  $F_{sz_i} = F_{sz_{il}} + F_{sz_{ir}}$ , ( $i = \{f, r\}$ ).

This model will be used in simulation for validation purpose (see Section IV). Note that the main interest in using the full vehicle model is that it allows to take into account nonlinear load transfer, slipping and side slip angles that are essential phenomena entering in the tire force, and consequently, in the global chassis dynamic, especially in dangerous driving situations.

### B. Suspensions model

Suspensions are usually modeled by a spring and a damping element. In real vehicles, their characteristics are nonlinear (see e.g. [7], [8]). Here, as long as we mainly focus on the longitudinal, lateral and yaw behaviors, without loss of generality, we will assume linear stiffness and damping coefficients. The suspension model adopted here is then given by:

$$F_{sz_{ij}} = k_{ij}(z_{s_{ij}} - z_{us_{ij}}) + c_{ij}(\dot{z}_{s_{ij}} - \dot{z}_{us_{ij}}) \quad (2)$$

### C. Tires model

Wheel and tire/road contact modeling is complex to achieve and is still a wide research area (see e.g. [9], [10]). Based on results given in [10], we propose the following tire models.

1) *Longitudinal tire model*: The longitudinal Burkhart model is given as (3) (see also [10]),

$$F_{tx_{ij}} = (\mu_1(1 - e^{-\lambda_{ij}\mu_2}) - \lambda_{ij}\mu_3)F_{n_{ij}} \quad (3)$$

where  $[\mu_1, \mu_2, \mu_3]$  gives the longitudinal road friction shape according to the considered road condition and  $F_{n_{ij}} = -F_{tz_{ij}} + g(m_{us_{ij}} + m_s/4)$  holds for the normal load at each corner of the vehicle.

2) *Lateral tire model*: The lateral force is given by formulae (4)

$$F_{ty_{ij}} = D e^{-6|\lambda_{ij}|^5} \sin(C \arctan(B(1-E)\beta_{ij} + E \arctan(B\beta_{ij}))) \quad (4)$$

where,  $\beta_{fj} = \beta_f = -\beta_{cog} - l_f \frac{\dot{\psi}}{v_x} + \delta$  and  $\beta_{rj} = \beta_r = -\beta_{cog} + l_r \frac{\dot{\psi}}{v_x}$  are the front and rear side slip angle respectively. Then  $B = (2 - \mu)b_t$ ,  $C = (5/4 - \mu/4)c_t$ ,  $D = d_t\mu$  and  $E = e_t$  are the lateral tire parameters, function of  $\mu \in [0; 1]$ , the tire/road adhesion coefficient. Additionally,  $e^{-6|\lambda_{ij}|^5}$  is used to model the fact that lateral friction forces are decreasing when slipping occurs (e.g. when vehicle is slipping, it is no longer manoeuvrable) then,  $\lim_{\lambda_{ij} \rightarrow |1|} F_{ty_{ij}} = 0$

3) *Vertical tire model*: Finally, the vertical forces are linearly described by (5),

$$F_{tz_{ij}} = k_{t_{ij}}(z_{us_{ij}} - z_{r_{ij}}) + c_{t_{ij}}(\dot{z}_{us_{ij}} - \dot{z}_{r_{ij}}) \quad (5)$$

### D. Actuators dynamic

In the paper, the considered actuators are the EMB, which allows to provide a continuously variable modulation braking torque, and an AS, that is simply an electric motor mounted on the column direction. These actuators will be modeled as first order low-pass transfer functions:

- The EMB actuators, providing the braking torque are modeled as,

$$\dot{T}_{br_j} = \varpi(T_{br_j}^0 - T_{br_j}) \quad (6)$$

where,  $\varpi = 70rd/s$  is the actuator cut-off frequency,  $T_{br_j}^0$  and  $T_{br_j}$  are the braking controller and actuator outputs respectively. In this paper, only the rear braking system is used to avoid coupling phenomena occurring with the steering system and because it affects more the vehicle yaw behavior than the front one.

- The AS actuator providing an additional steering angle is modeled as,

$$\dot{\delta}^+ = \kappa(\delta^0 - \delta^+) \quad (7)$$

where,  $\kappa = 10rd/s$  is the actuator cut-off frequency,  $\delta^0$  and  $\delta^+$  are the steering controller and actuator outputs respectively. This actuator is bounded between  $[-5, +5]$  degrees.

$$\left\{ \begin{array}{l} \dot{v}_x = -(F_{tx_f} \cos(\delta) + F_{tx_r} + F_{ty_f} \sin(\delta))/m - \dot{\psi}v_y \\ \dot{v}_y = (-F_{tx_f} \sin(\delta) + F_{ty_r} + F_{ty_f} \cos(\delta))/m + \dot{\psi}v_x \\ \ddot{z}_s = -(F_{sz_f} + F_{sz_r} + F_{dz})/m_s \\ \ddot{z}_{us_{ij}} = (F_{sz_{ij}} - F_{tz_{ij}})/m_{us_{ij}} \\ \ddot{\theta} = ((F_{sz_{rl}} - F_{sz_{rr}})t_r + (F_{sz_{fl}} - F_{sz_{fr}})t_f + mh\dot{v}_y)/I_x \\ \ddot{\phi} = (F_{sz_f}l_f - F_{sz_r}l_r - mh\dot{v}_x)/I_y \\ \ddot{\psi} = (l_f(-F_{tx_f} \sin(\delta) + F_{ty_f} \cos(\delta)) - l_r F_{ty_r} + (F_{tx_{fr}} - F_{tx_{fl}})t_f \cos(\delta) - (F_{tx_{rr}} - F_{tx_{rl}})t_r + M_{dz})/I_z \\ \dot{\omega}_{ij} = (R_{ij}F_{tx_{ij}} - T_{b_{ij}}^f)/I_w \\ \dot{\beta}_{cog} = (F_{ty_f} + F_{ty_r})/(mv_x) + \dot{\psi} \end{array} \right. \quad (1)$$

### III. MAIN RESULT: GCC STRUCTURE AND SYNTHESIS

This Section is devoted to the description of the main result of this paper, namely, the synthesis of a multivariable Global Chassis Controller (GCC) involving steering and rear braking actuators.

#### A. Global chassis control structure and working principle

The objective is to improve handling and safety by using the rear braking actuators and to activate the front steering system when braking is not efficient enough to achieve the required performance level.

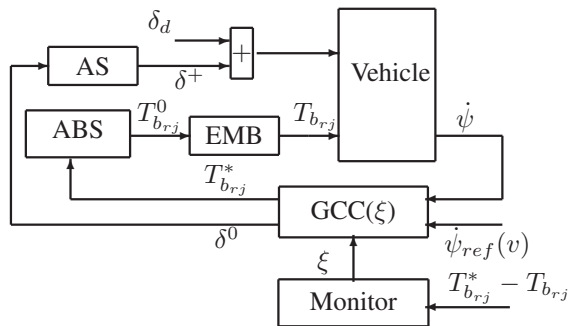


Fig. 1. The global integrated control structure.

Figure 1 shows the proposed global control structure including the following blocks:

- **Vehicle & Actuators (AS & EMB):** are the full nonlinear vehicle and actuator models (see Section II)
- **GCC( $\xi$ ):** is the proposed global chassis controller (see subsection III-B) providing the desired braking torque ( $T_{br,j}^*$ ) and the additive steering angle ( $\delta^0$ ), scheduled by  $\xi$ , the monitoring parameter
- **ABS:** is the local control implemented on each of the rear wheels (see subsection III-C) that is activated when rear slipping occurs, and that provides  $T_{br,j}^0$ , the braking torque, according to the set point ( $T_{br,j}^*$ ) provided by the GCC( $\xi$ ) bloc (based on [6])
- **Monitor:** is the scheduling strategy (see subsection III-D) that supervises the GCC( $\xi$ )

Then the so called GCC, using parameter dependent performance weighting functions, is synthesized in the LPV/ $\mathcal{H}_\infty$  framework using the brake efficiency measure ( $\xi$ ) as the

scheduling variable. Each block is then described in the following subsections.

#### B. LPV generalized plant and LPV/ $\mathcal{H}_\infty$ GCC synthesis

The idea is to synthesize a GCC that generates a stabilizing reference moment  $M_{dz}^*$  to achieve handling performances and to ensure passenger safety when dangerous situations are detected and provide an additive steering angle  $\delta^+$  when braking is no longer efficient to guarantee safety.

*Remark 1:* To convert the stabilizing moment reference ( $M_{dz}^*$ ) into effective braking torque, the following transformation has to be done:

$$T_{br,l}^* = \frac{RM_{dz}^*}{t_r} \text{ and } T_{br,r}^* = -\frac{RM_{dz}^*}{t_r} \quad (8)$$

Remember that the braking torque is bounded as  $T_{br,j} \in \mathcal{T}_b$ , where  $\mathcal{T}_b := \{T_b \in \mathbb{R} : 0 \leq T_b \leq T_{b,max}\}$ .

First, the generalized plant used for synthesis is introduced, then, one describes the LPV/ $\mathcal{H}_\infty$  solution to design a Dynamical Output Feedback (DOF) stabilizing controller that minimizes the  $\mathcal{H}_\infty$  norm for LPV system using a polytopic approach is described through Linear Matrix Inequalities (LMIs).

1) *LPV generalized plant model for synthesis:* First, let introduce the extended bicycle model given in equation (9), used for synthesis.

To fit with the robust framework, one considers the following weighting functions, and the generalized plant given in Figure 2:

- $W_{e_\psi} = 10 \frac{s/500+1}{s/50+1}$ , that is used to shape the yaw rate error ( $e_\psi = \psi_{ref} - \dot{\psi}$ )
- $W_{\dot{v}_y} = 10^{-3}$ , that attenuates the lateral acceleration
- $W_{M_{dz}^*} = 10^{-5} \frac{s/10\varpi+1}{s/100\varpi+1}$ , that attenuates the yaw moment control input
- $W_{\delta^0}(\xi) = \xi \frac{s/\kappa+1}{s/10\kappa+1}$ , that attenuates the steering control input according to  $\xi$

Note that the weight on the steering actuators (namely  $W_{\delta^+}(\xi)$ ) is linearly parameterized by the considered varying parameter  $\xi(\cdot) \in \mathcal{P}_\xi$ , where  $\mathcal{P}_\xi$  is defined as  $\mathcal{P}_\xi := \{\xi \in \mathbb{R} : \underline{\xi} \leq \xi \leq \bar{\xi}\}$  (where  $\underline{\xi} = 0.1$  and  $\bar{\xi} = 10$ ). Then when  $\xi = \bar{\xi}$ , the steering input is penalized, on the contrary, when  $\xi = \underline{\xi}$ , the steering control signal is no more penalized.

$$\begin{bmatrix} \dot{\psi}_y \\ \dot{\psi} \\ \dot{\beta} \end{bmatrix} = \begin{bmatrix} 0 & l_r C_{yr} - l_f C_{yf} - v & \frac{C_{yr} - C_{yf}}{m} \\ 0 & -\frac{l_f^2 m v}{l_r C_{yr} - l_f C_{yf}} + l_r^2 C_{yr} & \frac{l_r C_{yr} - l_f C_{yf}}{m} \\ 0 & -1 + \frac{l_r C_{yr} - l_f C_{yf}}{m v^2} & -\frac{l_f C_{yf} + C_{yr}}{m v} \end{bmatrix} \begin{bmatrix} v_y \\ \psi \\ \beta \end{bmatrix} + \begin{bmatrix} \frac{C_{yf}}{m} \\ -\frac{l_f C_{yf}}{m v} \\ \frac{C_{yf}}{m v} \end{bmatrix} \delta^* + \begin{bmatrix} 0 \\ \frac{1}{I_z} \\ 0 \end{bmatrix} M_{dz}^* + \begin{bmatrix} -\frac{1}{m} \\ 0 \\ \frac{1}{m v} \end{bmatrix} F_{dy} \quad (9)$$

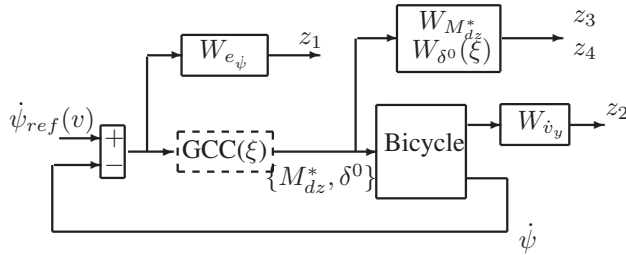


Fig. 2. Generalized plant for synthesis.

As the generalized plant is LPV, it can be modeled as,

$$\Sigma(\xi) : \begin{bmatrix} \dot{x} \\ z \\ y \end{bmatrix} = \begin{bmatrix} A(\xi) & B_1(\xi) & B_2 \\ C_1(\xi) & D_{11}(\xi) & D_{12} \\ C_2 & 0 & 0 \end{bmatrix} \begin{bmatrix} x \\ w \\ u \end{bmatrix} \quad (10)$$

where  $x$  includes the state variables of the system and of the weighing functions,  $w = F_{dy}$  and  $u = [\delta^0, M_{dz}^*]$  are the exogenous and control inputs respectively;  $z = [z_1, z_2, z_3, z_4] = [W_{e_\psi} e_\psi, W_{\dot{\psi}_y} \dot{\psi}_y, W_{M_{dz}^*} M_{dz}^*, W_{\delta^0(\xi)} \delta^0]$  holds for the controlled output, and  $y = \dot{\psi}_{ref}(v) - \dot{\psi}$  is the system measure ( $\dot{\psi}_{ref}(v)$  is provided by a reference nonlinear bicycle model and fed by  $\delta_d$ ). The LPV system (10) can be described as a polytopic system, i.e. a convex combination of the systems defined at each vertices formed by  $\mathcal{P}_\xi$ , namely  $\Sigma(\xi)$  and  $\Sigma(\bar{\xi})$ .

2) *LMI based LPV/ $\mathcal{H}_\infty$  polytopic solution:* The DOF-LPV/ $\mathcal{H}_\infty$  problem consists in finding a stabilizing controller, scheduled by  $\xi$ , of the form,

$$S(\xi) : \begin{bmatrix} \dot{x}_c \\ u \end{bmatrix} = \begin{bmatrix} A_c(\xi) & B_c(\xi) \\ C_c(\xi) & 0 \end{bmatrix} \begin{bmatrix} x_c \\ y \end{bmatrix} \quad (11)$$

that minimizes the  $\mathcal{H}_\infty$  norm of the closed-loop LPV system formed by the interconnection of (10) and (11) at each vertex. Finding such a controller can be done by applying the well known Bounded Real Lemma (BRL) to LPV systems. An LMI solution for polytopic systems consists in solving the following problem at each vertex of the polytope formed by the system as described thereafter.

*Proposition 1:* LMI based LPV/ $\mathcal{H}_\infty$  controller synthesis According to system (10), and via the change of basis expressed in [11], a non-conservative LMI (12) that expresses the same problem as the BRL can be formulated and solved by a Semi-Definite Program (SDP). Applied to the LPV polytopic problem, it consists in solving LMI (12) at each vertex formed by the LPV system, by using a common Lyapunov function, i.e. a common  $X > 0$  and  $Y > 0$ . The problem consists in finding  $\tilde{A}$ ,  $\tilde{B}$  and  $\tilde{C}$  at each vertex. Then the controller reconstruction is obtained solving the

following system at each vertex:

$$\begin{cases} \tilde{C} = C_c M^T \\ \tilde{B} = N B_c \\ \tilde{A} = Y A X + N B_c C_c X + Y B_2 C_c M^T + N A_c M^T \end{cases}$$

where  $N$  and  $M$  are defined by the designer so that  $M N^T = I - X Y$ .

By solving (12) for the LPV system (10) using Yalmip interface [12] and SeDuMi solver [13], one obtains  $\gamma = 2.48$  and the following controller Bode diagrams (Figure 3).

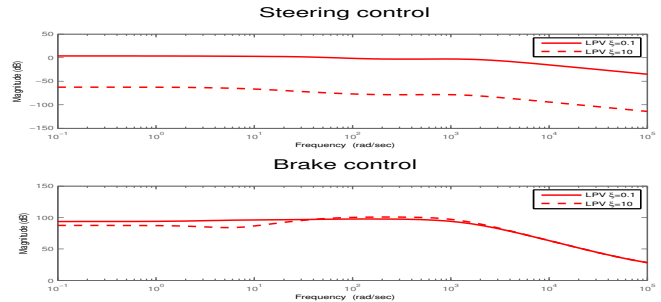
Fig. 3. Bode diagrams of the controller outputs  $\delta^+$  and  $M_{dz}^*$ 

Figure 3 shows the steering and braking controller output according to  $\xi$ . As the steering weight has been described as parameter dependent, we see that when  $\xi = \bar{\xi} = 10$ , steering signal is attenuated, and, conversely, when  $\xi = \xi = 0.1$  steering gain is larger. As a consequence, (see also Section IV), when  $\xi$  is low (resp. high), steering is activated (resp. deactivated). Intermediate values will give intermediate behaviors. Remember that, since  $\xi \in \mathcal{P}_\xi$ , the closed loop stability is guaranteed (thanks to the LPV design).

### C. Local rear ABS controller

As previously introduced (see also Figure 1), a local ABS controller is used at each rear wheel to achieve good braking and avoid slipping (leading to loss of manoeuvrability). Since the GCC synthesis is performed assuming linear tire stiffness, a local controller is essential to prevent from too high braking torque that would lead to slipping situations. In this paper we use the ABS sliding-mode based control law given in [6], [14] which exhibits good robustness properties w.r.t. actuator bandwidth, road type and measurement noise and allows to handle the compromise between wheel deceleration low performance and poor slip estimation. This local design is applied to each rear wheels and provides  $T_{b_{ABS_{r,j}}}$ . To be integrated to the proposed GCC structure, one just modifies the control law as:

$$T_{b_{r,j}} = \min(T_{b_{ABS_{r,j}}}, T_{b_{r,j}}^*) \quad (13)$$

$$\begin{bmatrix} \mathbf{AX} + \mathbf{XA}^T + \mathbf{B}_2\tilde{\mathbf{C}} + \tilde{\mathbf{C}}^T\mathbf{B}_2^T & (*)^T & (*)^T & (*)^T \\ \tilde{\mathbf{A}} + \mathbf{A}^T & \mathbf{YA} + \mathbf{A}^T\mathbf{Y} + \tilde{\mathbf{B}}\mathbf{C}_2 + \mathbf{C}_2^T\tilde{\mathbf{B}}^T & (*)^T & (*)^T \\ \mathbf{B}_1^T & \mathbf{B}_1^T\mathbf{Y} + \mathbf{D}_{21}^T\tilde{\mathbf{B}}^T & -\gamma\mathbf{I}_m & (*)^T \\ \mathbf{C}_1\mathbf{X} + \mathbf{D}_{12}\tilde{\mathbf{C}} & \mathbf{C}_1 & \mathbf{D}_{11} & -\gamma\mathbf{I}_q \end{bmatrix} < 0 \text{ and } \begin{bmatrix} \mathbf{X} & \mathbf{I}_n \\ \mathbf{I}_n & \mathbf{Y} \end{bmatrix} > 0 \quad (12)$$

#### D. Monitor: braking efficiency measure

The aim of the monitor is to schedule the GCC control to activate the steering system when braking is no longer efficient enough to guarantee safety. Then, one proposes the following scheduling strategy:

$$e = \max(|e_{T_{brj}}|), j = \{l, r\} \quad (14)$$

where  $e_{T_{brj}} = T_{b_{ABSrj}} - T_{brj}^*$ , and one defines the scheduling parameter  $\xi(e)$  as:

$$\xi := \begin{cases} \bar{\xi} & \text{if } e \leq \underline{\chi} \\ \frac{\bar{\chi} - e - \bar{\xi}}{\bar{\chi} - \underline{\chi}}\bar{\xi} + \frac{e - \underline{\chi}}{\bar{\chi} - \underline{\chi}}\underline{\xi} & \text{if } \underline{\chi} < e < \bar{\chi} \\ \underline{\xi} & \text{if } e \geq \bar{\chi} \end{cases} \quad (15)$$

where  $\underline{\chi} = \frac{30}{100}T_{b_{max}}$  and  $\bar{\chi} = \frac{70}{100}T_{b_{max}}$  are user defined brake efficiency measures. Note that other monitor strategies may be employed.

#### IV. NONLINEAR SIMULATION RESULTS

To validate the proposed GCC, a double line change manoeuvre is simulated on the full nonlinear model introduced in Section II. Both simulations are performed on a wet road, with a vehicle initial speed of  $100\text{km/h}$ .

- 1) First, the simulation is performed without faulty actuator (Figures 4-left and 5)
- 2) Secondly, a faulty rear left braking system is considered (Figures 4-right and 6)

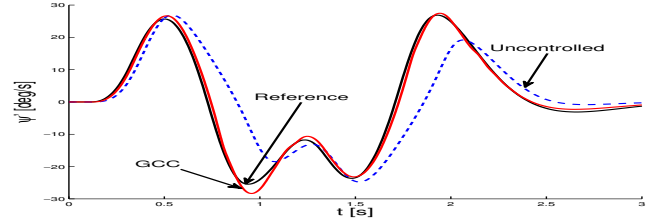
##### A. Double line change (healthy actuator)

As the road is wet, road/tire adhesion is low and lateral tire contact forces are strongly diminished. As a consequence, during the manoeuvre, the uncontrolled vehicle derives away from the desired path (see Figure 4-left).

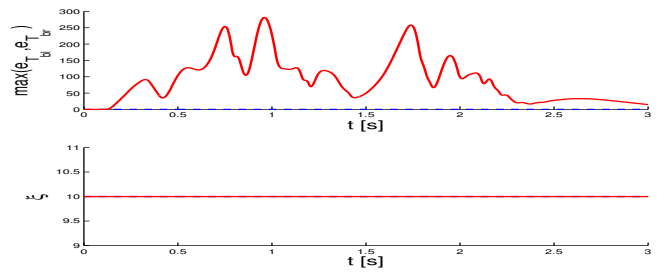
By comparing the yaw rate behaviors given in Figure 5-(a), it is clear that the proposed integrated control scheme enhances vehicle stability comparing to the non controlled one. Then, Figure 5-(b) shows that the scheduling parameter  $\xi$  does not vary since the braking system is efficient enough to stabilize the vehicle. Consequently, the control signal only involves the braking system (see Figure 5-(c)) and the steering control input is almost not activated ( $|\delta^0| < 10^{-3}$  degree).

##### B. Double line change (faulty actuator)

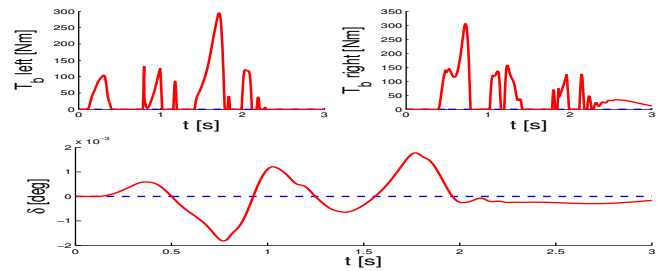
Here a fault occurs on the rear left braking during the same critical driving situation. Now, the maximal braking torque that can be applied by the rear left braking actuator is bounded by  $50\text{Nm}$  (the healthy maximal torque is  $1200\text{N}$ ). Then, the vehicle path is given on Figure 4-right.



(a) Yaw rate ( $\psi$ ).



(b) Scheduling parameter ( $\xi$ ), function of  $\max(|e_{T_{brj}}|)$ .



(c) Control signals ( $\delta^0$  and  $T_{brj}^0$ ).

Fig. 5. Simulation of a double line change manoeuvre on a wet road with initial speed  $v_0 = 100\text{km/h}$ .

As in the previous situation, the handling is clearly improved. Then comparing yaw rate curves (Figure 6-(a)), one can appreciate the improvement brought by the LPV control structure. As the rear right braking system is faulty when the vehicle would need it, from  $t = 1.5\text{s}$  to  $t = 2.1\text{s}$ , the GCC controller is scheduled to activate the steering system to counteract the undesired behavior (Figure 6-(b,c)). Especially, one note that the  $\xi$  parameter, according to (15), diminishes during this period (from 10 to 4, Figure 6-(b)) activating in the same time the steering input (Figure 6-(c)).

#### V. CONCLUSION AND DISCUSSION

The aim of this work is to enhance vehicle safety in critical driving situations. For that purpose, a reconfigurable Global Chassis Controller (GCC) structure involving braking and steering subsystems has been proposed. The control structure

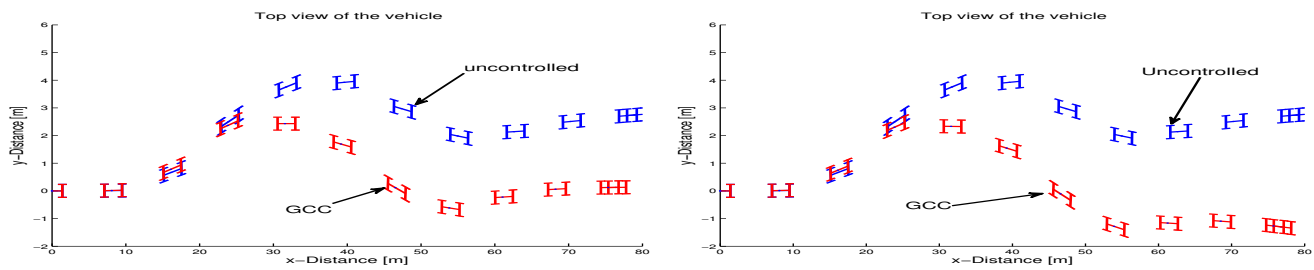


Fig. 4. Vehicle path after a double line change manoeuvre on a wet road ( $v_0 = 100\text{km/h}$ ) without (with) a fault on the rear left actuator, left (right).

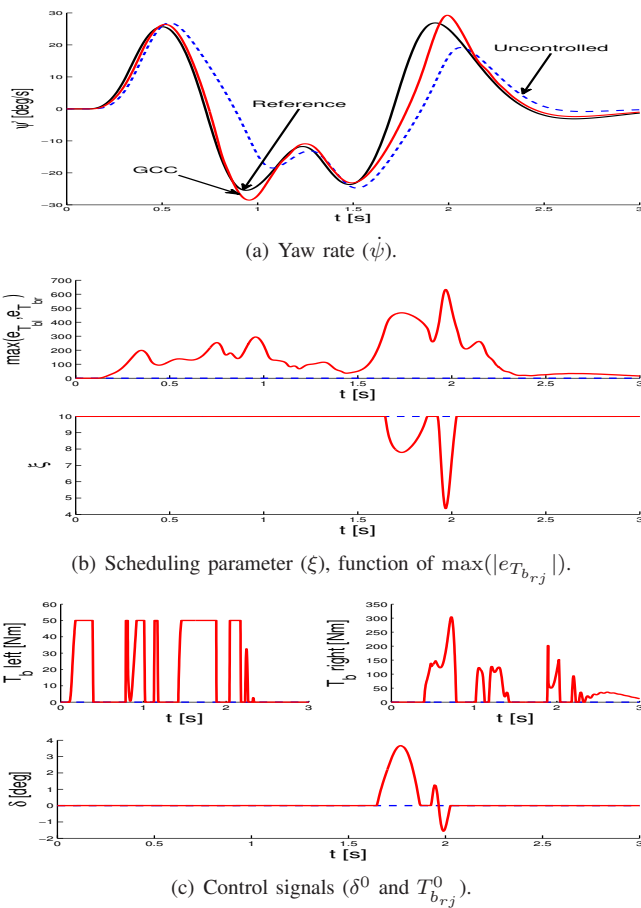


Fig. 6. Simulation of a double line change manoeuvre on a wet road with initial speed  $v_0 = 100\text{km/h}$  with a fault on the rear left actuator.

consists in scheduling the controller (with  $\xi$ , a braking efficiency measure) to solve the dynamical problem by the use of differential braking, and, if necessary the intervention of the steering actuator. This parameter dependent structure is synthesized in the LPV/ $\mathcal{H}_\infty$  framework, which guarantees the closed-loop stability and performances for all variations of the parameter in the defined convex set (here,  $\xi \in \mathcal{P}_\xi$ ). As the proposed GCC solution is integrated in a vehicle dynamic framework, the obtained controller shows to be robust to fault occurring on the braking system and to critical driving situations. Moreover, as long as the general structure does not involve any optimization process, it shows to be

easy to implement on real vehicles, even those where local ABS are already working well (as an illustration, here, the proposed GCC is well integrated with existing ABS strategy [6]). Simulations of critical driving situations show the effectiveness of the proposed control design. Further simulations and descriptions are available in [15].

## REFERENCES

- [1] P. Gáspár, Z. Szabó, and J. Bokor, "The design of an integrated control system in heavy vehicles based on an LPV method," in *Proceedings of the 44th IEEE Conference on Decision and Control (CDC)*, Seville, Spain, December 2005, pp. 6722–6727.
- [2] J. Andreasson and T. Bunte, "Global chassis control based on inverse vehicle dynamics models," *Vehicle System Dynamics*, vol. 44, no. supplement, pp. 321–328, 2006.
- [3] H. Chou and B. D'Andréa-Novel, "Global vehicle control using differential braking torques and active suspension forces," *Vehicle System Dynamics*, vol. 43, no. 4, pp. 261–284, April 2005.
- [4] P. Falcone, F. Borrelli, J. Asgari, H. Tseng, and D. Hrovat, "Predictive active steering control for autonomous vehicle systems," *IEEE Transaction on Control System Technology*, vol. 15, no. 3, pp. 566–580, May 2007.
- [5] P. Gáspár, Z. Szabó, J. Bokor, C. Poussot-Vassal, O. Sename, and L. Dugard, "Toward global chassis control by integrating the brake and suspension systems," in *Proceedings of the 5th IFAC Symposium on Advances in Automotive Control (AAC)*, Aptos, California, USA, August 2007.
- [6] M. Tanelli, R. Sartori, and S. Savaresi, "Combining slip and deceleration control for brake-by-wire control systems: a sliding-mode approach," *European Journal of Control*, vol. 13, no. 6, pp. 593–611, december 2007.
- [7] A. Zin, O. Sename, P. Gaspar, L. Dugard, and J. Bokor, "Robust LPV -  $\mathcal{H}_\infty$  control for active suspensions with performance adaptation in view of global chassis control," *Vehicle System Dynamics*, vol. 46, no. 10, pp. 889–912, October 2008.
- [8] C. Poussot-Vassal, O. Sename, L. Dugard, P. Gáspár, Z. Szabó, and J. Bokor, "New semi-active suspension control strategy through LPV technique," *Control Engineering Practice*, vol. 16, no. 12, pp. 1519–1534, December 2008.
- [9] M. Denny, "The dynamics of antilock brake systems," *European Journal of Physics*, vol. 26, pp. 1007–1016, 2005.
- [10] U. Kiencke and L. Nielsen, *Automotive Control Systems*, Springer-Verlag, Ed., 2000.
- [11] C. Scherer, P. Gahinet, and M. Chilali, "Multiobjective output-feedback control via LMI optimization," *IEEE Transaction on Automatic Control*, vol. 42, no. 7, pp. 896–911, july 1997.
- [12] J. Lofberg, "YALMIP : A toolbox for modeling and optimization in matlab," in *Proceedings of the CACSD Conference*, 2004.
- [13] J. F. Sturm, "Using SeDuMi 1.02, a MATLAB toolbox for optimization over symmetric cones," *Optim. Methods Softw.*, vol. 11/12, no. 1-4, pp. 625–653, 1999, interior point methods.
- [14] S. Savaresi, M. Tanelli, and C. Cantoni, "Mixed slip-deceleration control in automotive braking systems," *ASME Transactions: Journal of Dynamic Systems, Measurement and Control*, vol. 129, no. 1, pp. 20–31, 2007.
- [15] C. Poussot-Vassal, "Robust multivariable linear parameter varying automotive global chassis control," PhD Thesis, Grenoble INP, GIPSA-lab, Grenoble, France, September 2008.